



Apatinib enhances the anti-tumor effect of paclitaxel via the PI3K/p65/Bcl-xl pathway in triple-negative breast cancer

Jing Chen¹, Shuzhen Deng², Yifan Zhang¹, Chaokun Wang¹, Xiaochen Hu¹, Dejiu Kong¹, Gaofeng Liang², Xiang Yuan¹, Yuanpei Li³, Xinshuai Wang¹

¹Henan Key Laboratory of Cancer Epigenetics, Cancer Hospital, The First Affiliated Hospital, College of Clinical Medicine, Medical College of Henan University of Science and Technology, Luoyang, China; ²School of Basic Medical Sciences, Henan University of Science and Technology, Luoyang, China; ³Department of Biochemistry and Molecular Medicine, UC Davis Comprehensive Cancer Center, University of California Davis, CA, USA

Contributions: (I) Conception and design: X Wang, Y Li; (II) Administrative support: S Deng, G Liang; (III) Provision of study materials or patients: X Yuan, Y Zhang; (IV) Collection and assembly of data: X Hu, D Kong; (V) Data analysis and interpretation: J Chen, C Wang; (VI) Manuscript writing: All authors; (VII) Final approval of manuscript: All authors.

Correspondence to: Xinshuai Wang. Henan Key Laboratory of Cancer Epigenetics, Cancer Hospital, The First Affiliated Hospital, College of Clinical Medicine, Medical College of Henan University of Science and Technology, Luoyang 471003, China. Email: xshuaiw@haust.edu.cn; Yuanpei Li. Department of Biochemistry and Molecular Medicine, UC Davis Comprehensive Cancer Center, University of California Davis, Sacramento 95817, CA, USA. Email: lypli@ucdavis.edu.

Background: Apatinib is a new generation of small molecule tyrosine kinase inhibitor, which can highly selectively inhibit phosphorylation of vascular endothelial growth factor receptor 2 (VEGFR-2). This study aimed to investigate the synergistic effects of apatinib and paclitaxel (PTX) on triple-negative breast cancer (TNBC) *in vivo* and *in vitro*, and to explore the molecular mechanism of the PI3K/p65/Bcl-xl pathway.

Methods: *In vitro*, 3-(4,5-dimethylthiazol-2-yl)-2,5-diphenyltetrazolium bromide (MTT) method, flow cytometry (FCM), wound healing assay, and transwell matrix assay were conducted to measure the effects of apatinib and PTX on cell viability, apoptosis, migration, and invasion in TNBC cell line MDA-MB-468. Western blot (WB) was conducted to detect protein expression levels of PI3K, p65, and Bcl-xl after the application of apatinib and PTX. *In vivo*, MDA-MB-468 tumor-bearing nude mice were treated with apatinib and PTX, and tumor growth was observed.

Results: *In vitro*, apatinib and PTX could synergistically suppress the cell viability, the combined group had the most obvious effect. Apatinib and PTX could promote apoptosis and suppress migration and invasion of TNBC cells. Apatinib could reduce the expression of p-PI3K, p65, and Bcl-xl proteins ($P < 0.05$). *In vivo*, apatinib and PTX could inhibit tumor size and weight of model mice, and the combined agents had a more significant effect.

Conclusions: Apatinib could enhance the anti-tumor effect of PTX on TNBC cells through the PI3K/p65/Bcl-xl molecular pathway, and apatinib combined with PTX might be a promising option for TNBC treatment.

Keywords: Apatinib; paclitaxel (PTX); PI3K/p65/Bcl-xl pathway; triple-negative breast cancer (TNBC)

Submitted Dec 23, 2020. Accepted for publication Jun 04, 2021.

doi: 10.21037/atm-21-805

View this article at: <https://dx.doi.org/10.21037/atm-21-805>

Introduction

Breast cancer (BC) is the most common malignancy among women in the world. In most developing countries, the incidence of BC has been on the rise for decades. In recent years, with the change of lifestyle and environmental factors, the incidence of BC is increasing in China, 3–8% patients are diagnosed with metastatic breast cancer (MBC) at their first physical assessment (1-3). With the development of economy and change of lifestyle, the risk factors leading to the occurrence and development of BC have permeated all aspects of general human life and work. The incidence and mortality rates of BC are expected to increase in tandem with these risk factors. Using immunohistochemical method BC can be divided into the following types: luminal A, luminal B, HER-2 overexpression, and triple-negative (4-6). Triple-negative breast cancer (TNBC) is defined as a subtype of breast cancer in which estrogen receptor (ER), progesterone receptor (PR) and human epidermal growth factor receptor-2 (HER-2) are all negative, and TNBC accounts for about 10.4–16.3% of the total BC (7). More common in young and pre-menopausal women, TNBC has an increased likelihood of being invasive and metastatic (8,9). There is no obvious curative effect on TNBC with endocrine therapy and anti-HER-2 drug therapy, and there is currently no specific treatment. The main treatment options include surgery, chemotherapy, and radiotherapy (10). Most commonly, chemotherapy with paclitaxel (PTX), platinum, and capecitabine comprises the main medical treatment method (11-13). However, about 30–40% of TNBC patients will display metastasis after therapy (14). Therefore, new treatment methods are needed to improve patient outcomes and prognosis.

Targeted therapy has recently gained attention due to its high specificity and lower side effects compared to traditional treatment methods. The growth of malignant tumors is accompanied by the formation of neovascularization, which plays an important role in the absorption of nutrition (15). Vascular endothelial growth factor (VEGF) and vascular endothelial growth factor receptor (VEGFR) signaling are crucial to cell proliferation and cancer progression (16). The proliferation and migration of tumor cells is induced by VEGF in combination with its receptor VEGFR (16-18), which usually exists in endothelial cells. Evidence has shown that VEGFR-2 can exist in different tumor types including Kaposi sarcoma, melanoma, ovarian cancer, head and neck squamous cell carcinoma, and BC (19-21), and that it has

the most specific effect on the angiogenesis of tumors. Phosphorylation of VEGFR-2 will cause signal cascade reaction, activate downstream molecular signal pathways, and trigger subsequent cell proliferation and migration and endothelial cell survival effects (3,22). Therefore, a research hotspot has emerged around reducing the death rate of TNBC patients by applying effective drugs for VEGFR-2.

Apatinib is a new generation of small molecule tyrosine kinase inhibitor, which belongs to anti-vascular targeted therapy drugs. It can highly selectively act on VEGFR-2 by inhibiting its phosphorylation (3,23), inhibit signal transmission of downstream molecular pathways, and cause apoptosis of tumor cells (24,25). Clinical tests (26,27) have confirmed that apatinib can prolong overall survival (OS) and progression-free survival (PFS) of patients with advanced gastric cancer. In addition, *in vitro* studies on related cell levels have shown that apatinib has the effects of inhibiting proliferation and inducing apoptosis of BC cell lines. Paclitaxel (PTX), the most widely used anticancer drug, is applied for the treatment of various types of malignant diseases. And PTX is frequently used as the first-line treatment drug in breast cancer (BC) (28,29). The anti-microtubule drug PTX is a traditional first-line drug for BC. And the research of paclitaxel and apatinib is of profound significance in the field of triple-negative breast cancer research. Therefore, in this study, we investigated the synergistic effects of apatinib and PTX on TNBC *in vivo* and *in vitro*, and explored the molecular mechanism of the PI3K/p65/Bcl-xl pathway. In this study, a protocol was prepared before the study without registration. We present the following article in accordance with the ARRIVE reporting checklist (available at <https://dx.doi.org/10.21037/atm-21-805>).

Methods

This study was approved by the Ethics Committee of the First Affiliated Hospital, and College of Clinical Medicine of Henan University of Science and Technology, in compliance with the National institutes of Health Guide for the Care and Use of Laboratory Animals.

Cell lines and reagents

Human TNBC MDA-MB-468 cells were obtained from the Laboratory of Cancer Epigenetics of the First Affiliated hospital of Henan University of Science and Technology. A total of 24 specific pathogen free (SPF) BALB/c nude female

mice, aged 4–5 weeks, were purchased from Changzhou Cavens Experimental Animal Co., Ltd. (Changzhou, Jiangsu, China). Apatinib was provided by Hengrui Pharmaceutical Co. Ltd. (Lianyungang, Jiangsu, China). Injections of PTX were obtained from Yangzijiang Pharmaceutical Group Co. Ltd. Dulbecco's modified eagle medium (DMEM) was purchased from Hyclone (Logan, UT, USA). The MTT [3-(4,5-dimethyl-2-thiazolyl)-2,5-diphenyl-2-H-tetrazolium bromid] assay, and other chemicals were purchased from Sigma-Aldrich (St. Louis, MO, USA). Anti-PI3K, anti-p-PI3K, anti-p65, and anti-Bcl-xl antibodies were purchased from Bioss Antibodies (Beijing, China).

MTT assay

Cell viability and the cytotoxic effects of apatinib, PTX, and apatinib combined with PTX against MDA-MB-468 cells were generally evaluated by MTT assay. Cells were plated in 96-well flat-bottomed microtiter plates (5×10^3 cells/well) overnight. The cells were then treated with various concentrations of drugs as indicated for another 48 h. Next, MTT working solutions were added in each well and incubated for another 4 h before the plate reading. The results are shown as the average cell viability [(retreat - OD_{blank})/(OD_{control} - OD_{blank}) × 100%] of triplicate wells.

Flow cytometry (FCM)

Annexin V and propidium iodide (PI) double staining was used to evaluate the MDA-MB-468 cell apoptosis treated with free apatinib and PTX, apatinib (2 μmol/L), PTX (0.2 μmol/L) and the two drugs. In short, 1×10^6 MDA-MB-468 cells were seeded into a 6-well plate overnight. Cells were treated with various concentrations of drugs for 24 h respectively. The cells were then harvested and stained with 10 μg/mL Annexin V-fluorescein isothiocyanate (FITC)/PI (Pharmingen, CA, USA). Cells were stained with 50 μg/mL PI and 100 μg/mL RNase A and were protected from light. Samples were evaluated by flow cytometer and results were analyzed using the software Flow Jo v7.6.1 (<https://www.flowjo.com/solutions/flowjo>).

Wound healing assay

An MDA-MB-468 wound healing model was established to assess whether tumor cells had migration ability *in vitro*. As time passed, the cells were expected to grow and impact

the scratch width. Migration distance was detected to determine the migration and repair effect of MDA-MB-468 compared with phosphate buffered saline (PBS) group after the application of apatinib and PTX. We selected 4 of the 6-well plates and MDA-MB-468 cells were inoculated into the 4-well (1×10^6 /mL). A sterilizing gun head was used to mark 3 cell scratches vertically and evenly. The 4-well were respectively added with serum-free medium, serum-free medium with 2 μmol/L of apatinib, serum-free medium with 0.2 μmol/L PTX and the two drugs. Photos were taken of the same site in each well at 0 and 48 h. Finally, calculate the healing area of cells in different drug pores were calculated, and the data were statistically analyzed. A microscope (TE2000-U, Nikon, Tokyo, Japan) was used to obtain images at 10× magnification.

Transwell assay

Complete medium was replaced with serum-free medium for 24–48 h to remove the influence of serum on the experimental results, and the solid Matrigel glue was transferred to a refrigerator at 4 °C. A total of 4 transwell cells were placed in 24-well plates. Matrigel glue at a concentration of 50 mg/L and PBS were diluted according to a ratio of 1:5, the upper chamber surfaces at the bottom of the transwell chamber were coated one by one, and air-dried on ice for about 1 h. The MDA-MB-468 cells were digested, centrifuged, and resuspended with sterile PBS 3 times to remove the influence of serum, and serum-free medium was added to limit the cell density to 1×10^6 /mL. Cell suspension was added to the bottom of the 4 cells, and 10^5 cells were added to each well. A combination of PBS, 2.0 μmol/L apatinib, 0.2 μmol/L PTX and the two drugs were added to the 4 wells, respectively. After 24 h, the cells were fixed with formaldehyde for 1–2 h. They were then placed at room temperature with 0.1% crystal violet for 30 mins. After washing, the cells were observed under a microscope. In each sample, 10 fields were randomly selected, the number of cells passing through the matrix glue was counted, the average value was calculated, and images were taken. Images were obtained at 4× magnification under the microscope (TE2000-U, Nikon, Tokyo, Japan).

Western blot (WB)

After specific treatment with free apatinib and PTX, apatinib, PTX and the combined apatinib and PTX, proteins were extracted using a lysis buffer from 1×10^6 cells and the protein concentration was determined using the

Bio-Rad Bradford protein assay (Nazareth Eke, Belgium). Equal amounts of proteins from each sample (20 µg) were denatured at 95 °C for 5 min and were subsequently loaded onto a 10% sodium dodecyl sulfate polyacrylamide gel electrophoresis (SDS-PAGE) gel. After separation, the proteins were transferred onto polyvinylidene fluoride (PVDF) membrane for 2 h at 400 mA. The transferred membrane was incubated with the appropriate primary antibodies including PI3K, p-PI3K, p65, Bcl-xl, and β-actin at 4 °C overnight. Next, the membranes were incubated with horseradish peroxidase-labeled, isotype-specific secondary anti-body (1:2,000) for 2 h at room temperature. The immune complexes were detected by enhancement with chemiluminescence substrate, and the level of proteins was quantified using Quantity One software (Bio-Rad Laboratories, Hercules, CA, USA). The gray value was measured by ImageJ software (<https://imagej.net/>), and the gray value/internal reference gray value of each strip was calculated.

Animal studies in vivo

Female BALB/c nude mice were purchased from Changzhou Cavens Experimental Animal Co. Ltd. (Changzhou, Jiangsu, China). The nude mice were raised in the SPF animal room of the First Affiliated Hospital of Henan University of Science and Technology. Sterile PBS solution was used to adjust the cell concentration to 5×10^6 cells/mL. The inoculation site was determined as the junction of the right back and right forelimb of the mice. When the tumor volume ($\text{length} \times \text{width}^2/2$) had reached about 150 mm³, the mice were randomly divided into 4 groups by random number method with 6 mice in each group based on general rules and treated with PBS, apatinib (50 mg/kg/day) orally daily, and/or PTX (10 mg/kg/week) by injection. And we marked the cage with a marker to prevent confusion. The researchers were aware of the group allocation at the different stages of the experiment. The day after medication was set as D0, and the length and width of the tumor and the weight of the mice were measured on D0, D4, D7, D11, D14, D17, and D21. We calculated the tumor volume ($\text{length} \times \text{width}^2/2$) and traced the data in the line chart. We weighed the body weight of tumor bearing nude mice by electronic balance and traced the data in another line chart. The mental state, water intake, and defecation of the mice were observed. On D21, the mice were sacrificed by cervical dislocation and the tumors were stripped for photographing, weighing, and length and width

measurement. Blood samples were collected for routine blood and biochemical testing. During the animal study, the nude mice would be excluded from the experiment if anyone of them died for any reason.

Statistical analysis

The experimental data were analyzed using the statistical software SPSS version 19.0 (IBM Corp., Armonk, NY, USA). Data are showed as mean standard error (SEM). Comparisons between multiple groups of data were made by one-way analysis of variance (ANOVA). Comparison between the two groups was tested by independent sample *t*-test. Statistical significance was considered at $P < 0.05$.

Results

Apatinib and PTX synergistically inhibited the cell viability in MDA-MB-468 cells

The MTT assay was performed to characterize the effect of apatinib or PTX on the viability of MDA-MB-468 cells. As displayed in *Figure 1A*, both apatinib and PTX exhibited significant cytotoxicity with half-maximal inhibitory concentrations (IC₅₀) of 20 and 2 µmol/L, respectively. Compared with PTX, apatinib significantly inhibited the cell viability in a concentration-dependent manner (*Figure 1B,C*). The combined regimens could reduce the survival rate of cells and significantly increase the survival inhibitory effect. The cytotoxic effects were strongest when both drugs were applied simultaneously, as shown in *Figure 1D*. In addition, the combined index (CI) values revealed that apatinib and PTX have synergistic inhibitory effects on MDA-MB-468 cells (*Figure 1E*). The bar graph showed that the higher the concentration of apatinib under the same concentration of paclitaxel, the lower the survival rate of MDA-MB-468 cells, and the higher the concentration of paclitaxel under the same concentration of apatinib, the lower the survival rate of MDA-MB-468 cells, too (*Figure 1F*). The results showed in *Figure 1F* were consistent with the results in *Figure 1B,C*.

Apatinib and PTX increased the apoptosis of MDA-MB-468 cells

As displayed in *Figure 2*, the apoptosis rates of the PBS, apatinib 2 µmol/L, and PTX 0.2 µmol/L groups were 2.49%±0.50%, 18.02%±0.66%, and 27.57%±0.34%, and

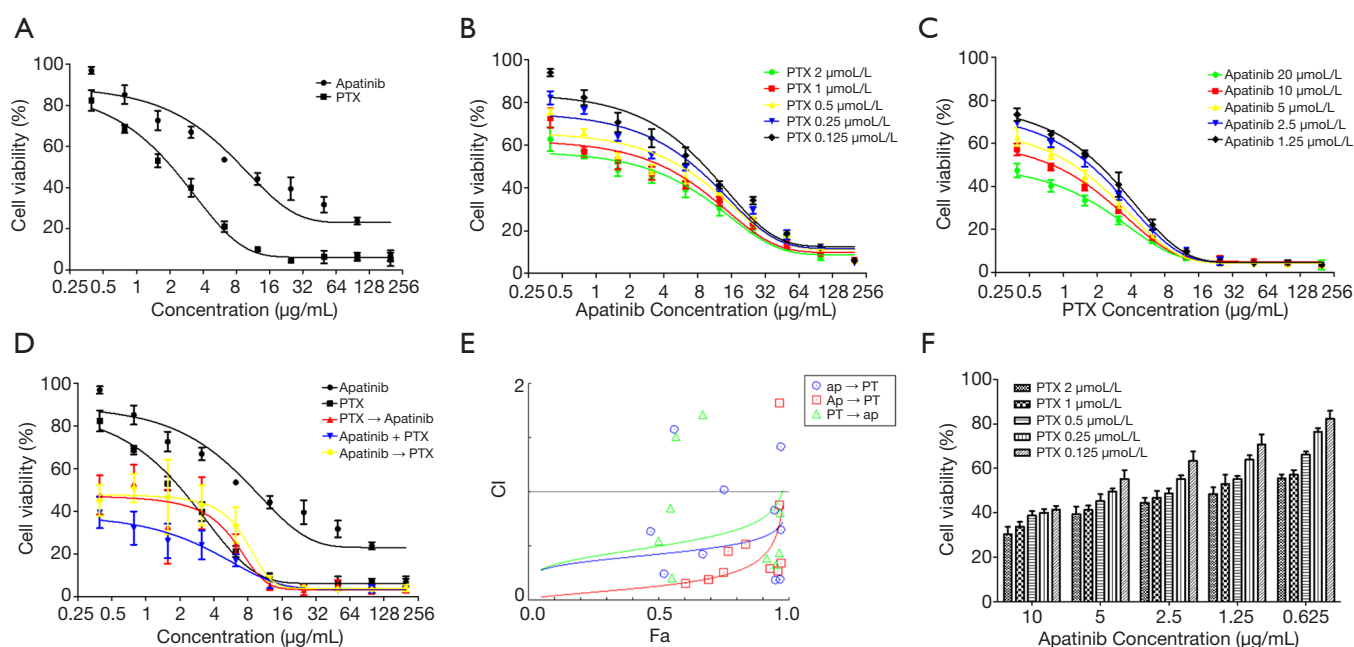


Figure 1 Anti-proliferative effects of apatinib and PTX on MDA-MB-468 cells. (A) Cell activity under 2 single drugs of apatinib and PTX. (B) The combination of apatinib and PTX: the concentration of apatinib in each plate was diluted, the concentration of PTX in the 5 plates was 2, 1, 0.5, 0.25, and 0.125 $\mu\text{mol/L}$, respectively. (C) The combination of apatinib and PTX: the concentration of PTX in each plate was diluted, the concentration of apatinib in the 5 plates was 20, 10, 5, 2.5, and 1.25 $\mu\text{mol/L}$, respectively. (D) Cell viability of the 2 monotherapies and 3 combined regimens. (E) The CI values of apatinib and PTX in the 3 combinations. (F) Histograms of the cell viability of apatinib and PTX. PTX, paclitaxel; CI, combined index.

$56.80 \pm 0.55\%$, respectively. These results indicated that apatinib and PTX could increase the apoptosis of MDA-MB-468 cells.

Apatinib and PTX decreased the wound healing and migration ability of MDA-MB-468 cells

The wound healing assay was employed to detect the mobility of cells under the influence of different drugs. The migration and wound healing ability of MDA-MB-468 cells decreased under the action of apatinib and PTX. The healing rates (%) were 50.69 ± 3.53 in the PBS group, 32.97 ± 2.87 in apatinib 2 $\mu\text{mol/L}$ group, 41.64 ± 2.72 in PTX 0.2 $\mu\text{mol/L}$ group, and 16.82 ± 2.93 in the combined group (Figure 3).

Apatinib and PTX reduced the invasive ability of MDA-MB-468 cells in vitro

The transwell assay was performed to detect the invasion ability of cells *in vitro* under the influence of apatinib and PTX. As shown in Figure 4A,B, the cell number

of MDA-MB-468 cells passing through the well in the PBS, apatinib (2 $\mu\text{mol/L}$), PTX (0.2 $\mu\text{mol/L}$) groups and the combined group were 701.33 ± 12.01 , 197.67 ± 21.03 ($P < 0.01$), 313.33 ± 13.05 ($P < 0.01$), and 117.33 ± 8.50 ($P < 0.01$), respectively. These results indicated that apatinib and PTX can reduce the invasive ability of MDA-MB-468 cells *in vitro*.

Apatinib down-regulated the expression of p-PI3K, p65, and Bcl-xl protein

WB was performed on the protein extracted from MDA-MB-468 cells treated with PBS, apatinib (2 $\mu\text{mol/L}$), apatinib (20 $\mu\text{mol/L}$), PTX (0.2 $\mu\text{mol/L}$), PTX (2 $\mu\text{mol/L}$) or the combined group with 20 $\mu\text{mol/L}$ apatinib and 2 $\mu\text{mol/L}$ PTX. The expression of PI3K, p-PI3K, p65, and Bcl-xl were examined. As displayed in Figure 5A, the expression of p-PI3K, p65, and Bcl-xl proteins were significantly down-regulated by apatinib. The protein expression of PI3K was not significantly different ($P > 0.05$) in Figure 5B. PTX down-regulated the expression of p-PI3K and Bcl-xl protein

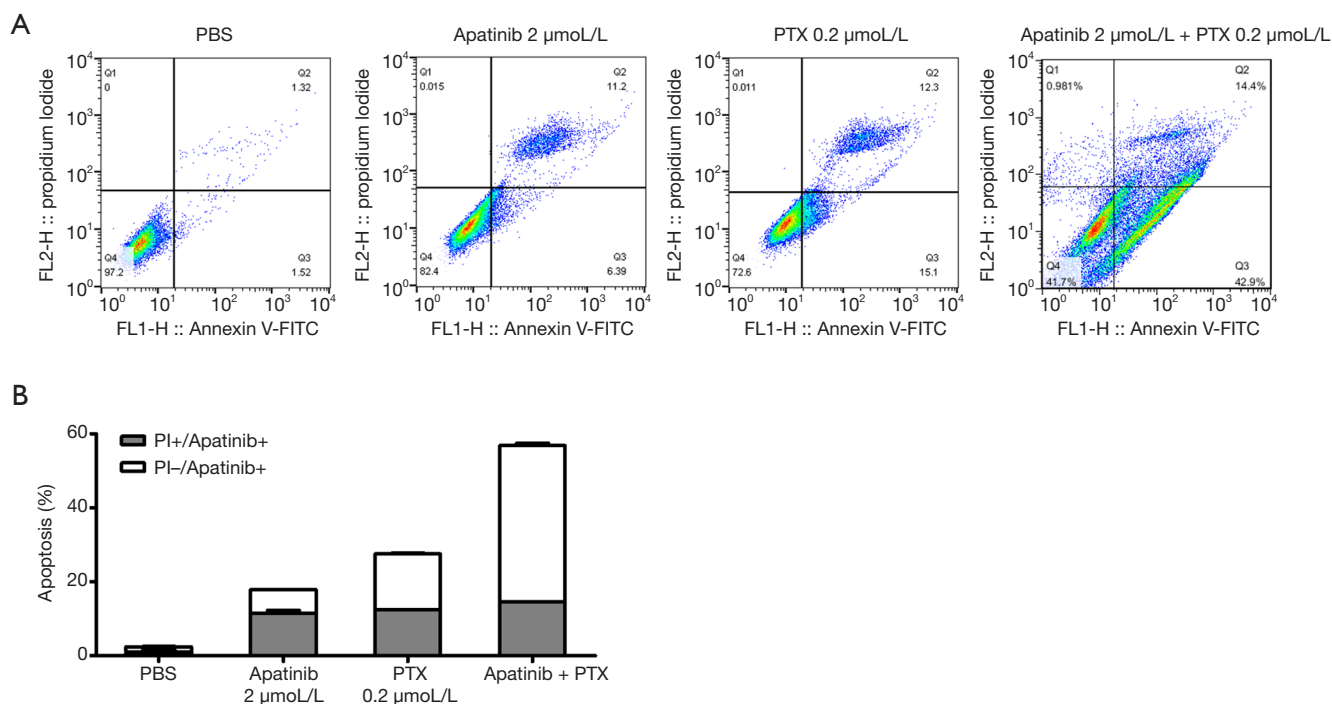


Figure 2 Cell apoptosis analysis of apatinib and PTX. (A) The proportion of different cell apoptosis of different cell apoptosis phases (Q1: necrotic cells; Q2: late apoptotic cells; Q3: early apoptotic cells; Q4: live cells) with free apatinib or PTX, apatinib 2 µmol/L, PTX 0.2 µmol/L and the two drugs. (B) The percentage of cells in different cell apoptosis phases is expressed in the histogram, and the data are presented as the mean and SE. PTX, paclitaxel; SE, standard error.

and up-regulated the expression of p65 protein (Figure 5B). And the expression of p-PI3K, p65, and Bcl-x1 protein were significantly down-regulated in the combined group with 20 µmol/L apatinib and 2 µmol/L PTX (Figure 5B).

Apatinib enhanced the anti-tumor effect of PTX in tumor mice in vivo

A total of 24 female nude mice carrying a tumor all survived after treatment with apatinib and PTX. There were 4 test groups assigned by our researchers, namely PBS, PTX, apatinib, and combined, and each group had 6 mice. There were no exclusions during the animal study. Tumor volume and weight, and mice body weight were observed during the experiment. As shown in Figure 6, the tumor weights at the endpoint of the experiment were 0.55 ± 0.21 g in PBS, 0.10 ± 0.15 g in PTX, 0.05 ± 0.02 g in apatinib, and 0.02 ± 0.01 g in the combined group. Apatinib, PTX, and the combination regimen could inhibit tumor growth, and the combined group had the most obvious effect. Tumor volume of the PBS group increased sharply during the experiment, but tumor

volume of the other three experimental groups decreased gradually after drug treatment, and the combined group displayed the most significant decrease in tumor volume. The body weight of mice in PBS group increased gradually, while the weight in the other 3 medication groups increased at a slower rate, and some weight loss was observed during the experimental period. The appetite and activity decreased in all groups except the PBS.

According to the results of routine blood and biochemical tests in Table 1, both apatinib and PTX caused reductions in white blood cells (WBC) index, and the reduction of WBC index in the combined group was statistically significant compared with the PBS group ($P < 0.05$). The alanine aminotransferase (ALT) and aspartate transaminase (AST) results of the apatinib monotherapy group were lower than those of the PBS group ($P < 0.05$).

Discussion

The incidence and mortality of BC malignant tumor are increasing year by year. The TNBC tumor type has a poor

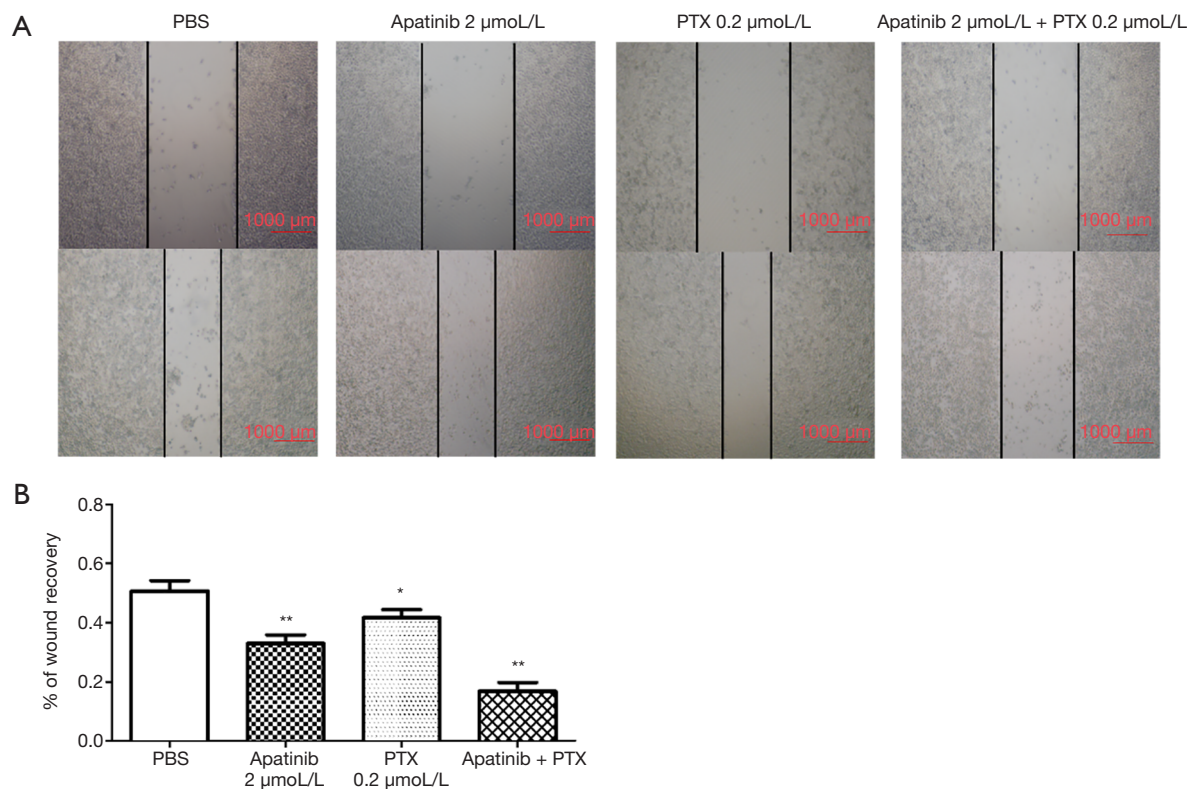


Figure 3 Effects of apatinib and PTX on damage repair in MDA-MB-468 cells. (A) Pictures of comparison of cell healing ability before and after treatment (with free apatinib or PTX; with apatinib 1 µg/mL; with PTX 0.2 µg/mL). (B) Histogram of percentage of wound recovery of PBS, apatinib 1 µg/ml, and PTX 0.2 µg/mL. Asterisks indicate significant differences when P values are <0.05 (*), <0.01 (**). PTX, paclitaxel; PBS, phosphate buffered saline.

prognosis, difficult treatment, poor long-term efficacy, which negatively impacts the quality of life of patients (30,31). This study investigated the effect of apatinib which selectively acts on VEGFR-2 apoptosis of TNBC based on the PI3K/p65/Bcl-xl molecular pathway. We compared apatinib with PTX, a traditional therapeutic drug, to further explore the effect of apatinib on inhibiting the growth and proliferation of TNBC tumors. After treatment with apatinib and PTX, cell viability decreased. The combination group was more potent than each single drug group, and the combination of apatinib and PTX had a synergistic effect on the survival inhibition of cancer cells. Apatinib and PTX could promote apoptosis of TNBC MDA-MB-468 cells. The two drugs were shown to affect the repair ability of cells after injury by decreasing cell movement and migration ability. The invasion ability also decreased after treatment with the two drugs. *In vivo*, apatinib and PTX inhibited tumor growth and slowed the rate of weight gain. The tumor volume and weight in the combined group were

smaller than the other three groups, indicating that the combined treatment had the strongest inhibitory effect on the growth of tumor cells. Concurrently, the mental state, activity, and appetite of nude mice in the drug treatment groups all decreased. The decrease in activity of nude mice was attributed to their mental state on the one hand, and it might also have been related to the tumor-burdened state and gradual growth of tumors. The results of routine blood and biochemical testing of the mice showed that the combined group had the most obvious effect of reducing WBC ($P < 0.05$). The levels of ALT and AST were also significantly decreased in the apatinib monotherapy group. The above experimental results show the combined group had the most significant therapeutic effect across many experiments. These effects may be related to the inhibition of downstream pathways caused by the interaction of apatinib and VEGFR-2. In addition, studies have confirmed that activation of the PI3K pathway may cause PTX resistance. Inhibition of the PI3K pathway could therefore

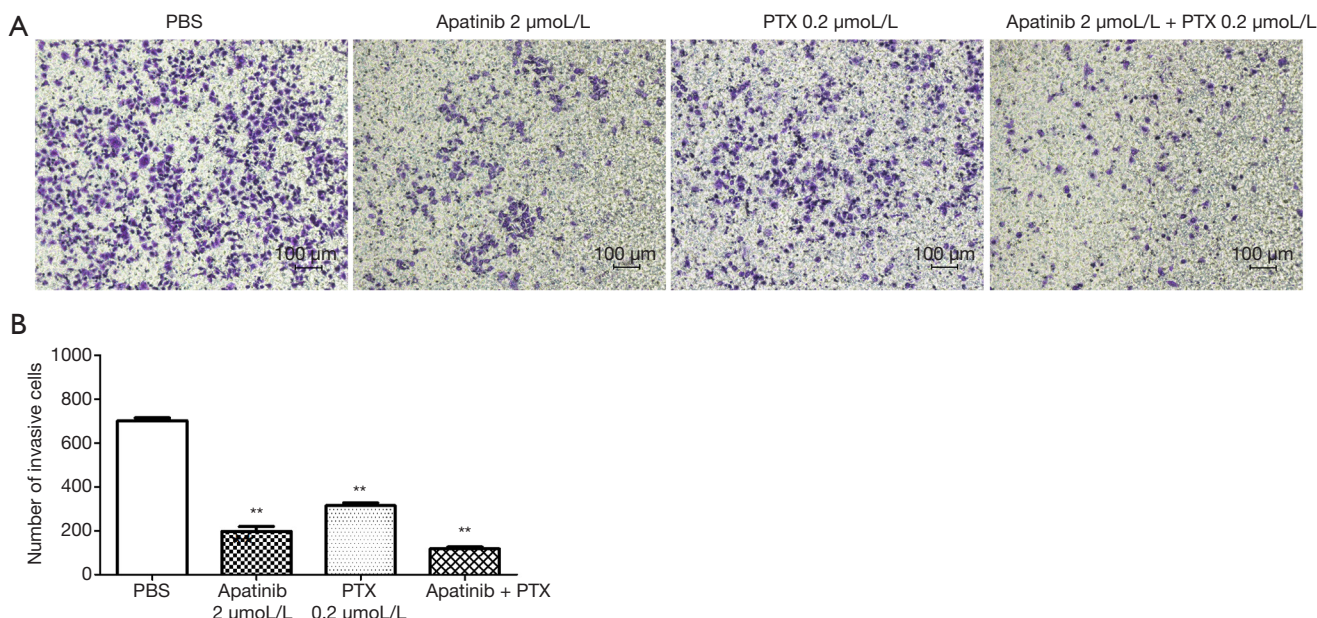


Figure 4 Effects of apatinib and PTX on cell invasion in MDA-MB-468 cells. (A) Pictures of invasive ability under different treatments (free apatinib or PTX; apatinib 2 μmol/L; PTX 0.2 μmol/L; apatinib 2 μmol/L + PTX 0.2 μmol/L). (B) Histogram of number of invasive cells of PBS, apatinib 2 μmol/L, PTX 0.2 μmol/L, and apatinib 2 μmol/L + PTX 0.2 μmol/L. Asterisks indicate significant differences when P values are <0.05 (*), <0.01 (**). PTX, paclitaxel; PBS, phosphate buffered saline.

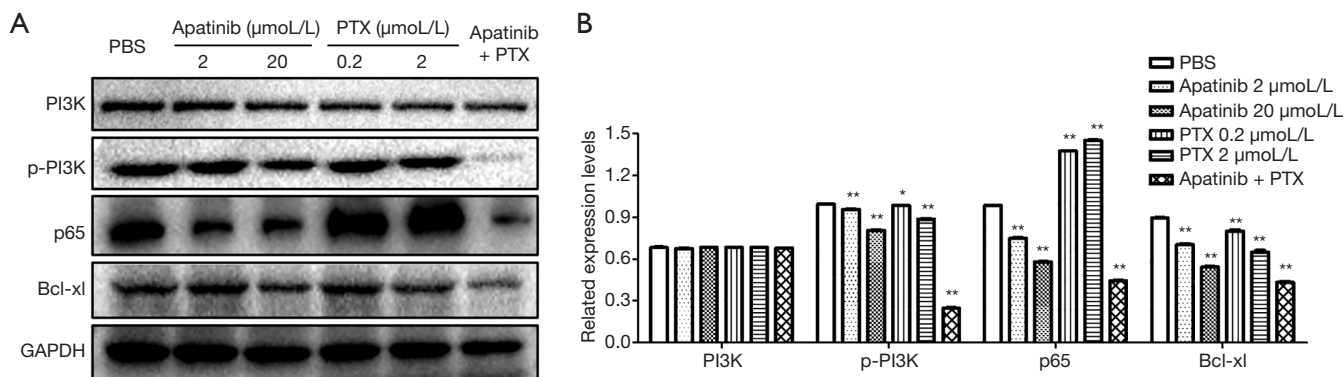


Figure 5 Expression of PI3K, p-PI3K, p65, and Bcl-xl proteins of MDA-MB-468 cells. (A) The picture of western blot using protein extracts after the treatment without apatinib or PTX, with apatinib 2 μmol/L, apatinib 20 μmol/L, PTX 0.2 μmol/L and PTX 2 μmol/L. (B) Histogram of protein expression after treatment of apatinib and PTX in different concentrations. Asterisks indicated significant differences when P values are <0.05 (*), <0.01 (**). PTX, paclitaxel.

reduce PTX resistance (32,33), making the treatment effect of apatinib combined with PTX more obvious.

WB results showed the trend of protein expression after drug administration at various concentrations. No significant changes in PI3K expression were observed after the application of apatinib at 0, 2, 20 μmol/L. The expressions

of p-PI3K, p65, and Bcl-xl all showed decreasing trends. Previous studies in human cholangiocarcinoma cells have shown that VEGFR-2 can activate the PI3K/protein kinase B (Akt) pathway to produce an anti-apoptosis effect (34). In this study, apatinib, as a drug that specifically acts on VEGFR-2, converted PI3K into PIP3 (the second signal-transmitting

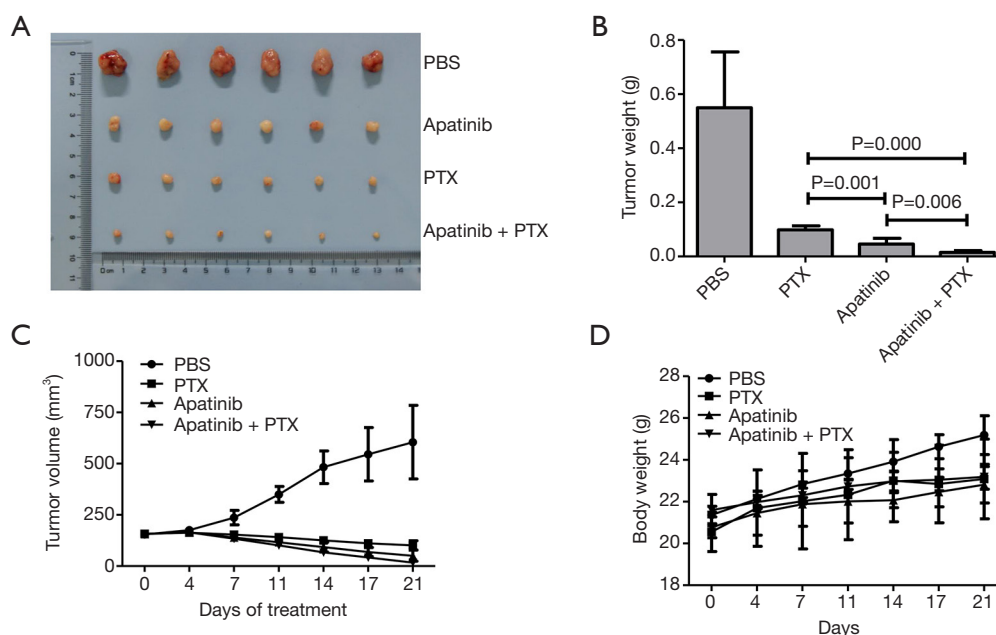


Figure 6 The synergistic therapeutic efficacy of apatinib and PTX in MDA-MB-468 TNBC xenograft model. (A) Tumors pictures obtained on day 21 after treatment. (B) Tumor weight obtained on day 21 after treatment. (C) Tumor growth ratio curve of tumor bearing nude mice treated with free apatinib or PTX, apatinib (50 mg/kg), PTX (10 mg/kg), or the combination of apatinib and PTX. (D) Change of body weight of tumor bearing nude mice during 21 days of medication. PTX, paclitaxel; TNBC, triple negative breast cancer.

Table 1 Effects of drugs on routine blood and liver and kidney function in nude mice

Item	Index	Group			
		PBS	PTX	Apatinib	PTX + apatinib
Blood routine	WBC/($\times 10^9$)	4.95 \pm 0.83	4.17 \pm 0.71	4.39 \pm 0.57	3.62 \pm 0.25
	RBC/($\times 10^{12}$)	9.36 \pm 0.59	9.31 \pm 0.33	9.58 \pm 0.17	9.14 \pm 0.36
	HGB(g/L)	135.25 \pm 8.06	139.25 \pm 3.40	142.75 \pm 3.20	136.50 \pm 5.74
	HCT/%	40.68 \pm 2.54	41.38 \pm 1.68	42.48 \pm 0.78	41.20 \pm 1.32
	PLT/($\times 10^9$)	835.65 \pm 58.58	842.575 \pm 120.89	846.08 \pm 75.66	878.00 \pm 21.23
Blood biochemistry	ALT/(U/L)	45.25 \pm 8.77	31.25 \pm 8.54	24.75 \pm 5.25	46.50 \pm 5.80
	AST/(U/L)	192.75 \pm 26.40	190.00 \pm 29.44	119.00 \pm 28.65	124.00 \pm 10.68
	UREA/(mmol/L)	9.58 \pm 3.21	5.95 \pm 3.11	14.06 \pm 5.46	6.71 \pm 1.91
	CREA/(mmol/L)	97.50 \pm 19.89	86.24 \pm 17.28	146.375 \pm 49.20	73.44 \pm 10.69
	URCA/(μ mol/L)	247.25 \pm 96.73	185.00 \pm 51.96	243.75 \pm 97.76	167.75 \pm 15.33

PTX, paclitaxel; PBS, phosphate buffered saline; WBC, white blood cell; RBC, red blood cell; HGB, hemoglobin; HCT, hematocrit; PLT, platelet; ALT, alanine aminotransferase; AST, aspartate transaminase; CREA, creatinine; URCA, uric acid.

messenger) after receiving signal stimulation through specific binding with VEGFR-2 site. The action of PIP3 could activate Akt (PKB) and further inhibit nuclear factor kappa-light-chain-enhancer of activated B cells (NF- κ B)

from entering the nucleus (35-37). Inhibiting the activation of NF- κ B can reduce the expression of angiogenic factors and angiogenesis (38). In addition, it can also inhibit and reduce the expression of Bcl-xl as expression of Bcl-xl is also

regulated at the transcription level. Transcription factor NF- κ B can regulate the common motif of the promoter region of Bcl-xl. Activation of NF- κ B can promote the expression of Bcl-xl. The expression of Bcl-xl decreases with the inhibition of the expression of NF- κ B. As an anti-apoptosis gene, the decrease of Bcl-xl expression leads to cell apoptosis instead of continuous growth and proliferation, thus inhibiting tumor growth.

When PTX was administered at 0, 0.2, 2 μ mol/L, the expression PI3K did not change significantly. Expression of p-PI3K showed a decreasing trend. Expression of p65 showed an increasing trend and Bcl-xl expression showed a declining trend. As a traditional drug for the treatment of BC, PTX mainly inhibits tumor cells by binding tubulin and inhibiting cell mitosis. It can inhibit the PI3K/Akt signaling pathway, inhibit phosphorylation of PI3K to p-PI3K, and down-regulate expression of p-AKT (39). Studies have shown that PTX inhibits the PI3K/Akt signaling pathway, which can increase the permeability of mitochondrial inner membranes, accelerate the disintegration of mitochondrial membrane potential, and promote the release of a variety of apoptotic factors, such as increasing the expression of Bcl-2 and increasing cell apoptosis (40,41). This is consistent with the result of WB that the expression of p-PI3K in BC cells treated with PTX was reduced, as was the expression of anti-apoptosis gene Bcl-xl, which belongs to Bcl-2 family. The increased expression of NF- κ B p65 may be due to the activation of NF- κ B by PTX. Studies have shown that PTX can activate NF- κ B and promote apoptosis in solid tumors (42). Apatinib and PTX may have different mechanisms of promoting cancer cell apoptosis, but eventually they both inhibit the expression of anti-apoptosis gene Bcl-xl, thus achieve the effect of inhibiting tumor growth. To summarize, NF- κ B and Bcl-xl play an important role in the process of cell growth via the PI3K/Akt pathway, and the molecular mechanisms are complex. This study illustrated the possible role that apatinib played to enhance the anti-tumor effect of PTX via the PI3K/p65/Bcl-xl molecular mechanism in TNBC MDA-MB-468 cells. This study had some limitations. The results of cell experiments and nude mice experiments confirmed the combination of apatinib and PTX may produce a synergistic anti-tumor effect which provides a basis for clinical application. However, the clinical applicability depends on large-scale clinical trials to further verify its effectiveness. With the development of medicine, additional research is still required to explore

other possible related molecular pathways and contribute more value to the treatment of TNBC.

Conclusions

This study identified that apatinib could enhance the anti-tumor effect of PTX via the PI3K/p65/Bcl-xl pathway, thus impeding tumor growth of TNBC.

Acknowledgments

We are grateful for the support of the Medical Science and Technology project of Henan province and Henan Key Laboratory of Cancer Epigenetics (Henan University of Science and Technology).

Funding: This work was supported by the Medical Science and Technology project of Henan province ([XSW] 201504029). The funding body provided funds to cover experimental expenses, but had no role in the design of the study, collection, analysis, and interpretation of data, or in writing of the manuscript.

Footnote

Reporting Checklist: The authors have completed the ARRIVE reporting checklist Available at <https://dx.doi.org/10.21037/atm-21-805>

Data Sharing Statement: Available at <https://dx.doi.org/10.21037/atm-21-805>

Conflicts of Interest: All authors have completed the ICMJE uniform disclosure form (available at <https://dx.doi.org/10.21037/atm-21-805>). The authors have no conflicts of interest to declare.

Ethical Statement: The authors are accountable for all aspects of the work in ensuring that questions related to the accuracy or integrity of any part of the work are appropriately investigated and resolved. This study was approved by the Ethics Committee of the First Affiliated Hospital, and College of Clinical Medicine of Henan University of Science and Technology, in compliance with the National institutes of Health Guide for the Care and Use of Laboratory Animals.

Open Access Statement: This is an Open Access article distributed in accordance with the Creative Commons

Attribution-NonCommercial-NoDerivs 4.0 International License (CC BY-NC-ND 4.0), which permits the non-commercial replication and distribution of the article with the strict proviso that no changes or edits are made and the original work is properly cited (including links to both the formal publication through the relevant DOI and the license). See: <https://creativecommons.org/licenses/by-nc-nd/4.0/>.

References

1. Bray F, Ferlay J, Soerjomataram I, et al. Global cancer statistics 2018: GLOBOCAN estimates of incidence and mortality worldwide for 36 cancers in 185 countries. *CA Cancer J Clin* 2018;68:394-424.
2. Chen W, Zheng R, Baade PD, et al. Cancer statistics in China, 2015. *CA Cancer J Clin* 2016;66:115-32.
3. Zhang H. Apatinib for molecular targeted therapy in tumor. *Drug Des Devel Ther* 2015;9:6075-81.
4. Perou CM, Sørlie T, Eisen MB, et al. Molecular portraits of human breast tumours. *Nature* 2000;406:747-52.
5. Sørlie T, Perou CM, Tibshirani R, et al. Gene expression patterns of breast carcinomas distinguish tumor subclasses with clinical implications. *Proc Natl Acad Sci U S A* 2001;98:10869-74.
6. Sørlie T, Tibshirani R, Parker J, et al. Repeated observation of breast tumor subtypes in independent gene expression data sets. *Proc Natl Acad Sci U S A* 2003;100:8418-23.
7. Riva F, Bidard FC, Houy A, et al. Patient-Specific Circulating Tumor DNA Detection during Neoadjuvant Chemotherapy in Triple-Negative Breast Cancer. *Clin Chem* 2017;63:691-9.
8. Oakman C, Viale G, Di Leo A, et al. Management of triple negative breast cancer. *Breast* 2010;19:312-21.
9. Anders CK, Zagar TM, Carey LA, et al. The management of early-stage and metastatic triple-negative breast cancer: a review. *Hematol Oncol Clin North Am* 2013;27:737-49, viii.
10. Chen J, Jiang P, Wang HJ, et al. The efficacy of molecular subtyping in predicting postoperative recurrence in breast-conserving therapy: a 15-study meta-analysis. *World J Surg Oncol* 2014;12:212.
11. Gradishar WJ, Krasnojon D, Cheporov S, et al. Significantly longer progression-free survival with nab-paclitaxel compared with docetaxel as first-line therapy for metastatic breast cancer. *J Clin Oncol* 2009;27:3611-9.
12. Hamilton E, Kimmick G, Hopkins J, et al. Nab-paclitaxel/bevacizumab/carboplatin chemotherapy in first-line triple negative metastatic breast cancer. *Clin Breast Cancer* 2013;13:416-20.
13. Masuda N, Lee SJ, Ohtani S, et al. Adjuvant Capecitabine for Breast Cancer after Preoperative Chemotherapy. *N Engl J Med* 2017;376:2147-59.
14. Bianchini G, Balko JM, Mayer IA, et al. Triple-negative breast cancer: challenges and opportunities of a heterogeneous disease. *Nat Rev Clin Oncol* 2016;13:674-90.
15. Zhang Z, Ji S, Zhang B, et al. Role of angiogenesis in pancreatic cancer biology and therapy. *Biomed Pharmacother* 2018;108:1135-40.
16. Xia G, Kumar SR, Hawes D, et al. Expression and significance of vascular endothelial growth factor receptor 2 in bladder cancer. *J Urol* 2006;175:1245-52.
17. Narendran A, Ganjavi H, Morson N, et al. Mutant p53 in bone marrow stromal cells increases VEGF expression and supports leukemia cell growth. *Exp Hematol* 2003;31:693-701.
18. Koch S, Claesson-Welsh L, et al. Signal transduction by vascular endothelial growth factor receptors. *Cold Spring Harb Perspect Med* 2012;2:a006502.
19. Stallone G, Schena A, Infante B, et al. Sunitinib for Kaposi's sarcoma in renal-transplant recipients. *N Engl J Med* 2005;352:1317-23.
20. Chen H, Ye D, Xie X, et al. VEGF, VEGFRs expressions and activated STATs in ovarian epithelial carcinoma. *Gynecol Oncol* 2004;94:630-5.
21. Gunningham SP, Currie MJ, Han C, et al. VEGF-B expression in human primary breast cancers is associated with lymph node metastasis but not angiogenesis. *J Pathol* 2001;193:325-32.
22. Masood R, Cai J, Zheng T, et al. Vascular endothelial growth factor (VEGF) is an autocrine growth factor for VEGF receptor-positive human tumors. *Blood* 2001;98:1904-13.
23. Ding J, Chen X, Dai X, et al. Simultaneous determination of apatinib and its four major metabolites in human plasma using liquid chromatography-tandem mass spectrometry and its application to a pharmacokinetic study. *J Chromatogr B Analyt Technol Biomed Life Sci* 2012;895-896:108-15.
24. Cock-Rada AM, Medjkane S, Janski N, et al. SMYD3 promotes cancer invasion by epigenetic upregulation of the metalloproteinase MMP-9. *Cancer Res* 2012;72:810-20.
25. Li J, Wang H, Ke H, et al. MiR-129 regulates MMP9 to control metastasis of non-small cell lung cancer. *Tumour*

- Biol 2015;36:5785-90.
26. Li J, Qin S, Xu J, et al. Apatinib for chemotherapy-refractory advanced metastatic gastric cancer: results from a randomized, placebo-controlled, parallel-arm, phase II trial. *J Clin Oncol* 2013;31:3219-25.
 27. Xu J, Zhang Y, Jia R, et al. Anti-PD-1 Antibody SHR-1210 Combined with Apatinib for Advanced Hepatocellular Carcinoma, Gastric, or Esophagogastric Junction Cancer: An Open-label, Dose Escalation and Expansion Study. *Clin Cancer Res* 2019;25:515-23.
 28. Abu Samaan TM, Samec M, Liskova A, et al. Paclitaxel's Mechanistic and Clinical Effects on Breast Cancer. *Biomolecules* 2019;9:789.
 29. Wang P, Song D, Wan D, et al. Ginsenoside panaxatriol reverses TNBC paclitaxel resistance by inhibiting the IRAK1/NF- κ B and ERK pathways. *PeerJ* 2020;8:e9281.
 30. Jung Y, Lee SJ, Lee J, et al. Assessment of Quality of Life and Safety in Postmenopausal Breast Cancer Patients Receiving Letrozole as an Early Adjuvant Treatment. *J Breast Cancer* 2018;21:182-9.
 31. Downey LB. Adjuvant treatment of breast cancer in the elderly. Understanding and addressing the challenges. *Oncology (Williston Park)* 2008;22:286-93; discussion 297-8.
 32. Knuefermann C, Lu Y, Liu B, et al. HER2/PI-3K/Akt activation leads to a multidrug resistance in human breast adenocarcinoma cells. *Oncogene* 2003;22:3205-12.
 33. Roy HK, Olusola BF, Clemens DL, et al. AKT proto-oncogene overexpression is an early event during sporadic colon carcinogenesis. *Carcinogenesis* 2002;23:201-5.
 34. Peng H, Zhang Q, Li J, et al. Apatinib inhibits VEGF signaling and promotes apoptosis in intrahepatic cholangiocarcinoma. *Oncotarget* 2016;7:17220-9.
 35. Beck JT, Ismail A, Tolomeo C, et al. Targeting the phosphatidylinositol 3-kinase (PI3K)/AKT/mammalian target of rapamycin (mTOR) pathway: an emerging treatment strategy for squamous cell lung carcinoma. *Cancer Treat Rev* 2014;40:980-9.
 36. Jeong SJ, Pise-Masison CA, Radonovich MF, et al. Activated AKT regulates NF- κ B activation, p53 inhibition and cell survival in HTLV-1-transformed cells. *Oncogene* 2005;24:6719-28.
 37. Daragmeh J, Barriah W, Saad B, et al. Analysis of PI3K pathway components in human cancers. *Oncol Lett* 2016;11:2913-8.
 38. Safdari Y, Khalili M, Ebrahimzadeh MA, et al. Natural inhibitors of PI3K/AKT signaling in breast cancer: emphasis on newly-discovered molecular mechanisms of action. *Pharmacol Res* 2015;93:1-10.
 39. Ying L, Zhu Z, Xu Z, et al. Cancer Associated Fibroblast-Derived Hepatocyte Growth Factor Inhibits the Paclitaxel-Induced Apoptosis of Lung Cancer A549 Cells by Up-Regulating the PI3K/Akt and GRP78 Signaling on a Microfluidic Platform. *PLoS One* 2015;10:e0129593.
 40. Jie B, Zhang X, Wu X, et al. Neuregulin-1 suppresses cardiomyocyte apoptosis by activating PI3K/Akt and inhibiting mitochondrial permeability transition pore. *Mol Cell Biochem* 2012;370:35-43.
 41. Weiss JN, Korge P, Honda HM, et al. Role of the mitochondrial permeability transition in myocardial disease. *Circ Res* 2003;93:292-301.
 42. Xu Y, Xin Y, Diao Y, et al. Synergistic effects of apigenin and paclitaxel on apoptosis of cancer cells. *PLoS One* 2011;6:e29169.

(English Language Editor: J. Jones)

Cite this article as: Chen J, Deng S, Zhang Y, Wang C, Hu X, Kong D, Liang G, Yuan X, Li Y, Wang X. Apatinib enhances the anti-tumor effect of paclitaxel via the PI3K/p65/Bcl-xl pathway in triple-negative breast cancer. *Ann Transl Med* 2021;9(12):1001. doi: 10.21037/atm-21-805